ELSEVIER

Journal of Organometallic Chemistry 534 (1997) 221–227

Journal of Organometallic Chemistry

Diiron acetylide complexes: molecular structures of $[Fe_2(CO)_4(\mu\text{-}C{\equiv}CPh)(\mu\text{-}PPh_2)(\mu\text{-}dppm)]$ and $[Fe_2(CO)_3(Ph_2PC{\equiv}CPh)(\mu\text{-}C{\equiv}CPh)(\mu\text{-}PPh_2)(\mu\text{-}dppm)]$

Graeme Hogarth *, Simon P. Redmond

Chemistry Department, University College London, 20 Gordon Street, London WC1H 0AJ, UK

Received 4 November 1996

Abstract

The synthesis and X-ray crystal structures of two diiron acetylide complexes $[Fe_2(CO)_{4-n}(Ph_2PC{\equiv}CPh)_n(\mu\text{-}C{\equiv}CPh)(\mu\text{-}PPh_2)(\mu\text{-}dppm)]$ (**1**, $n = 0$; **2**, $n = 1$) are presented together with the synthesis of $[Fe_2(CO)_3\{P(OEt)_3\}(\mu\text{-}C{\equiv}CPh)(\mu\text{-}PPh_2)(\mu\text{-}dppm)]$ **3**; structural comparisons made with related phosphido-bridged diiron complexes are used to elucidate the role of ground state structural changes in the $\sigma{-}\pi$ acetylide fluxionality. © 1997 Elsevier Science S.A.

Keywords: X-ray crystal structure; Acetylide ligand; Diiron

1. Introduction

The acetylide ligand (C≡CR) has been widely studied at both mononuclear and polynuclear metal centres [1]. At the binuclear centre it is most commonly found acting in a bridging capacity, being σ-bound to one metal atom and π-bound to the second. This then differentiates the two metal sites in the solid state, however, in solution more often than not the acetylide moiety is highly fluxional, interconverting metal sites via a transition state in which the acetylide is linear [2]. Specifically, a range of diiron phosphido-bridged acetylide complexes prepared by Carty and coworkers [3] have been shown to be highly fluxional on the NMR timescale, the free energy of activation being sensitive to the nature of other substituents at iron. For example, the displacement of two carbonyls for bis(diphenylphosphino)methane (dppm) in $[Fe_2(CO)_6(\mu\text{-}C{\equiv}CBu^t)(\mu\text{-}PPh_2)]$ results in a decrease in $\Delta G^{\#}$ by approximately 1 Kcal mol^{-1} [4]. In closely related studies on the fluxionality of $\sigma{-}\pi$ alkenyl complexes we have found evidence attributing large changes in free energies of activation to small ground state differences in coordination of the organic moiety to the diiron centre [5]. In the light of these findings, we wondered whether analogous ground state structural changes in diiron acetylide complexes could account for observed changes in the free energy of acetylide fluxionality. Herein we report the X-ray crystal structures of two such complexes $[Fe_2(CO)_{4-n}(Ph_2PC{\equiv}CPh)_n(\mu\text{-}C{\equiv}CPh)(\mu\text{-}PPh_2)(\mu\text{-}dppm)]$ ($n = 0$, 1) and compare them with the related complexes $[Fe_2(CO)_{6-n}(PPh_3)_n(\mu\text{-}C{\equiv}CPh)(\mu\text{-}PPh_2)]$ ($n = 0$ [6], 1 [7]).

2. Experimental details

2.1. General comments

All reactions were carried out under N_2 in pre-dried solvents. NMR spectra were recorded on a Varian VXR spectrometer and IR spectra on a Nicolet 205 Fourier transform spectrometer. Chromatography was carried out on columns of deactivated alumina (6% w/w water). Photochemical reactions were carried out using a 500W Hanovia medium pressure mercury lamp. Elemental analyses were performed in the Chemistry Department of University College. Triethylphosphite was purchased from Aldrich and used without further purification,

* Corresponding author. E-mail: uccaxgh@ucl.ac.uk.

PII S0022-328X(96)06929-X

$Ph_2PC{\equiv}CPh$ was prepared by Dr. S. Doherty of the University of Newcastle following the literature procedure [8], while $[Fe_2(CO)_4(\mu\text{-}C{\equiv}CPh)(\mu\text{-}PPh_2)(\mu\text{-}dppm)]$ was also prepared as previously described [9].

2.2. Synthesis of $[Fe_2(CO)_3(Ph_2PC{\equiv}CPh)(\mu\text{-}C{\equiv}CPh)(\mu\text{-}PPh_2)(\mu\text{-}dppm)]$ 2

A toluene solution (100 cm^3) of **1** (250 mg, 0.28 mmol) and $Ph_2C{\equiv}CPh$ (100 mg, 0.35 mmol) was irradiated whilst slowly purging with nitrogen. After 12 h, a significant darkening of the orange solution was observed and the solvent was removed under reduced pressure. Chromatography eluting with dichloromethane–light petroleum (1:4) gave an orange band which afforded 40 mg of unreacted **1**. Further elution with dichloromethane–light petroleum (1:1) gave a red band which afforded a red solid shown by IR spectroscopy to contain both **1** and **2**. Crystallisation of the mixture upon slow diffusion of methanol into a concentrated dichloromethane solution afforded large red crystals of **2** (180 mg, 70%) and a small amount of orange crystals of **1** (ca. 10 mg). IR (CH_2Cl_2) (C≡C) 2180w, (CO) 1953vs, 1916vs, 1899s, 1879m cm^{-1}. ^1H NMR ($CDCl_3$) δ 8.0–6.5 (m, 50H, Ph), 3.46 (q, J 10.7, 1H, CH_2), 2.69 (dt, J 9.9, 5.8, 1H, CH_2). ^{13}C NMR ($CDCl_3$) 220.7 (m, 2CO), 219.8 (d, J 7.3, CO), 142–124 (m, Ph), 122.4 (s, PC≡*C*Ph), 105.3 (d, J 8.0, μ-*C*≡CPh), 100.7 (s, μ-C≡*C*Ph), 91.2 (d, J 30.0, P*C*≡CPh), 41.1 (t, J 22.5, CH_2) ppm. ^{31}P NMR ($CDCl_3$) 166.1 (ddd, J 137.2, 81.1, 29.9, μ-PPh_2), 67.5 (dd, J 81.1, 64.3, dppm), 60.9 (dd, J 137.2, 63.7, dppm), 55.5 (d, J 29.9, $Ph_2PC{\equiv}CPh$) ppm. Mass spectrum (FAB); m/e 1153, 1125, 1068, 782. Anal. Found: C, 66.15; H, 4.20. $Fe_2C_{68}H_{52}O_3P_4 \cdot CH_2Cl_2$ Calc.: C, 66.93; H, 4.36%.

2.3. Synthesis of $[Fe_2(CO)_3\{P(OEt)_3\}(\mu\text{-}C{\equiv}CPh)(\mu\text{-}PPh_2)(\mu\text{-}dppm)]$ 3

Thermolysis of a toluene solution (50 cm^3) of **1** (100 mg, 0.11 mmol) and $P(OEt)_3$ (100 mg, 0.60 mmol) for 4 h resulted in a very slight darkening of the solution. Removal of the solvent under reduced pressure gave an oily orange solid which was washed with hexane (2 × 5 cm^3) and dried. Chromatography eluting with dichloromethane–light petroleum (1:4) gave an orange band which afforded **3** (60 mg, 52%) as an orange powder. Attempts to crystallise **3** from a variety of solvents resulted in some decomposition as a result of phosphite loss. IR (CH_2Cl_2) ν(CO) 1957vs, 1917vs, 1893s, 1875sh cm^{-1}. ^1H NMR ($CDCl_3$) δ 8.1–6.7 (m,

Table 1
Crystallographic data

	1 · CH_2Cl_2	**2** · CH_2Cl_2
Formula	$Fe_2C_{50}H_{39}O_4P_3Cl_2$	$Fe_2C_{69}H_{54}O_3P_4Cl_2$
Space group	$P\bar{1}$	$P2_1/c$
a (Å)	12.286(2)	13.872(6)
b (Å)	12.347(4)	17.236(7)
c (Å)	18.179(7)	25.731(7)
α (deg)	76.06(3)	90
β (deg)	89.01(3)	104.53(3)
γ (deg)	61.23(2)	90
V (Å^3)	2330.3(12)	5956(4)
Z	2	4
F(000)	1004	2552
d_{calc} (g cm^{-3})	1.396	1.380
Crystal size (mm^3)	0.85 × 0.46 × 0.40	0.48 × 0.36 × 0.30
μ(Mo Kα) (cm^{-1})	8.84	7.32
Orientation refinements: no.; range	30; $18 \le 2\theta \le 28$	25; $17 \le 2\theta \le 27$
Data measured	8596	9699
Unique data	8185	9277
No. of unique data with $I \ge 2.0\sigma(I)$	6641	6164
No. of parameters	550	721
R [a], R_w [b] for $I \ge 2.0\sigma(I)$	0.0478, 0.0840	0.0468, 0.1136
R [a], R_w [b] for all data	0.0621, 0.1676	0.0651, 0.1258
Weighting scheme	$W^{-1} = \sigma^2(F) + 0.000000F^2$	$W^{-1} = \sigma^2(F) + 0.000759F^2$
Largest shift/e.s.d., final cycle	0.11	0.12
Largest peak, hole (e Å^{-3})	0.891, −0.844	0.524, −0.580

[a] $R = \Sigma[|F_o| - |F_c|]/\Sigma|F_o|$.
[b] $R_w = \Sigma w^{1/2} \cdot [|F_o| - |F_c|]/\Sigma w^{1/2} \cdot |F_o|$.

Table 2
Atomic coordinates ($\times 10^4$) and equivalent isotropic displacement parameters ($Å^2 \times 10^3$) for **1**

Atom	x	y	z	U_{eq}
Fe(1)	523(1)	6116(1)	7056(1)	34(1)
Fe(2)	2735(1)	5483(1)	7616(1)	32(1)
P(1)	−359(1)	8177(1)	7013(1)	33(1)
P(2)	2274(1)	7421(1)	7733(1)	33(1)
P(3)	2186(1)	4198(1)	7278(1)	37(1)
O(1)	592(3)	6678(3)	5411(2)	72(1)
O(2)	−1602(3)	5684(3)	7079(2)	82(1)
O(3)	3432(3)	6064(3)	6107(2)	59(1)
O(4)	5283(2)	3793(3)	8354(2)	67(1)
C(1)	564(3)	6450(3)	6057(2)	46(1)
C(2)	−772(3)	5864(3)	7080(2)	46(1)
C(3)	3138(3)	5845(3)	6703(2)	39(1)
C(4)	4268(3)	4469(3)	8087(2)	41(1)
C(5)	1080(3)	5730(3)	8094(2)	37(1)
C(6)	1773(3)	5251(3)	8696(2)	40(1)
C(7)	818(3)	8663(3)	7117(2)	37(1)
C(10)	−1282(3)	9288(3)	6111(2)	36(1)
C(11)	−1135(3)	10288(3)	5708(2)	49(1)
C(12)	−1897(4)	11093(4)	5028(2)	60(1)
C(13)	−2779(4)	10884(4)	4750(2)	57(1)
C(14)	−2934(4)	9889(4)	5142(2)	58(1)
C(15)	−2190(3)	9092(3)	5820(2)	51(1)
C(20)	−1444(3)	8840(3)	7695(2)	38(1)
C(21)	−1578(4)	8056(4)	8326(2)	53(1)
C(22)	−2316(4)	8581(5)	8872(3)	70(1)
C(23)	−2920(4)	9871(5)	8781(3)	77(1)
C(24)	−2808(4)	10663(4)	8145(3)	72(1)
C(25)	−2070(3)	10155(4)	7599(2)	54(1)
C(30)	3331(3)	8053(3)	7416(2)	36(1)
C(31)	2940(4)	9337(4)	7332(2)	58(1)
C(32)	728(5)	9833(4)	7076(3)	72(1)
C(33)	4892(4)	9053(5)	6912(3)	68(1)
C(34)	5287(4)	7794(4)	7002(2)	63(1)
C(35)	4505(3)	7290(4)	7251(2)	47(1)
C(40)	2080(3)	7670(3)	8679(2)	37(1)
C(41)	959(4)	8463(4)	8909(2)	49(1)
C(42)	887(5)	8551(4)	9662(2)	65(1)
C(43)	1938(5)	7866(5)	10174(2)	71(1)
C(44)	3068(5)	7069(4)	9955(2)	66(1)
C(45)	3140(4)	6968(4)	9216(2)	53(1)
C(50)	2822(3)	3507(3)	6486(2)	44(1)
C(51)	4067(4)	3047(4)	6389(3)	66(1)
C(52)	4536(5)	2563(5)	5773(3)	95(2)
C(53)	3760(6)	2553(5)	5248(3)	94(2)
C(54)	2527(5)	3000(5)	5340(3)	85(2)
C(55)	2052(4)	3467(4)	5958(2)	60(1)
C(60)	2290(4)	2828(3)	7998(2)	45(1)
C(61)	3439(4)	1857(4)	8365(3)	86(2)
C(62)	3537(6)	784(5)	8889(3)	107(2)
C(63)	2519(6)	661(5)	9043(3)	86(2)
C(64)	1387(6)	1597(5)	8675(3)	96(2)
C(65)	1271(4)	2682(4)	8156(3)	72(1)
C(70)	2150(3)	4818(3)	9513(2)	44(1)
C(71)	3337(4)	3858(4)	9838(2)	68(1)
C(72)	3641(5)	3506(5)	10621(3)	84(2)
C(73)	2758(6)	4111(6)	11076(3)	88(2)
C(74)	1574(5)	5030(5)	10760(2)	79(2)
C(75)	1271(4)	5387(4)	9979(2)	59(1)
C(100)	2149(7)	6232(7)	3885(4)	156(3)
Cl(1)	721(2)	7396(2)	3373(2)	187(1)
Cl(2)	3314(3)	6022(3)	3440(3)	318(3)

Note to Table 2:
U_{eq} is defined as one third of the trace of the orthogonalized U_{ij} tensor.

35H, Ph), 3.81 (m, 3H, OCH_2), 3.50 (m, 4H, OCH_2 + CH_2), 2.75 (dt, *J* 9.7, 5.6, 1H, CH_2), 1.09 (t, 9H, *J* 7.1, CH_3). ^{13}C NMR ($CDCl_3$) 221.0 (t, *J* 27.0, CO), 220.2 (d, *J* 10.5, CO), 220.1 (q, *J* 21.0, CO), 142–124 (m, Ph), 100.4 (d, *J* 8.7, μ-*C*≡CPh), 68.1 (s, μ-C≡*C*Ph), 59.9 (s, OCH_2), 40.7 (t, *J* 20.5, CH_2), 16.1 (s, CH_3) ppm. ^{31}P NMR ($CDCl_3$) 190.4 (dd, *J* 38.5, 16.6, $P(OEt)_3$), 171.4 (ddd, *J* 141.3, 78.2, 38.4, μ-PPh_2), 67.1 (ddd, *J* 78.9, 64.5, 15.4, dppm), 61.1 (dd, *J* 141.3, 65.0, dppm) ppm. Mass spectrum (FAB); *m/e* 1032, 975, 918, 782. Anal. Found: C, 56.32; H, 4.45. $Fe_2C_{54}H_{52}O_3P_4 \cdot 2CH_2Cl_2$ Calc.: C, 55.91; H, 4.66%.

2.4. Thermolysis of 2

Thermolysis of a xylene solution (20 cm^3) of **2** (30 mg, 0.026 mmol) for 2 h resulted in a lightening of the solution which was shown by IR spectroscopy to be primarily **1**. Chromatography afforded only **1** (16 mg, 66%).

2.5. X-ray data collection and solution

For both structures, a single crystal was mounted on a glass fibre and all geometric and intensity data were taken from this sample using an automated four-circle diffractometer (Nicolet R3mV) equipped with Mo-Kα radiation ($\lambda = 0.71073$ Å). Important crystallographic parameters are summarised in Table 1. The lattice parameters were identified by application of the automatic indexing routine of the diffractometer to the positions of a number of reflections taken from a rotation photograph and centred by the diffractometer. The ω–2θ (**1**) or ω (**2**) techniques were used to measure reflections in the range $5° \leq 2\theta \leq 50°$ (**1**) and $5° \leq 2\theta \leq 48°$ (**2**). Three standard reflections (remeasured every 97 scans) showed no significant loss in intensity during data collection. The data were corrected for Lorentz and polarisation effects and empirically for absorption. The unique data with $I \geq 2.0\sigma(I)$ were used to solve and refine the structures.

Structures were solved by direct methods and developed by using alternating cycles of least-squares refinement and difference Fourier synthesis. All non-hydrogen atoms were refined anisotropically. Hydrogens were placed in idealised positions (C–H 0.96 Å) and assigned a common isotropic thermal parameter ($U = 0.08$ $Å^2$). Final difference Fourier maps were featureless and contained no peaks greater than 1.00 e $Å^3$. Structure solution used the SHELXTL program package on an IBM PC [10].

Tables 2 and 3 give atomic coordinates and equivalent isotropic displacement parameters for **1** and **2** re-

Table 3
Atomic coordinates ($\times 10^4$) and equivalent isotropic displacement parameters ($Å^2 \times 10^3$) for **2**

Atom	x	y	z	U_{eq}
Fe(1)	2788(1)	2766(1)	1425(1)	31(1)
Fe(2)	3727(1)	1929(1)	2234(1)	32(1)
P(1)	3489(1)	3873(1)	1796(1)	33(1)
P(2)	4489(1)	2852(1)	2799(1)	33(1)
P(3)	2718(1)	1477(1)	1486(1)	35(1)
P(4)	1403(1)	3158(1)	868(1)	38(1)
O(1)	3914(2)	2643(2)	612(1)	61(1)
O(2)	4122(2)	435(2)	2772(1)	74(1)
O(3)	5432(2)	2106(2)	1779(1)	56(1)
C(1)	3461(3)	2711(2)	929(2)	41(1)
C(2)	3966(3)	1046(2)	2590(2)	44(1)
C(3)	4730(3)	2019(2)	1945(1)	38(1)
C(4)	2400(2)	2599(2)	2066(1)	34(1)
C(5)	2312(3)	2273(2)	2483(1)	40(1)
C(6)	380(3)	3304(2)	1151(2)	47(1)
C(7)	−293(3)	3370(2)	1366(2)	47(1)
C(8)	4547(3)	3720(2)	2390(1)	37(1)
C(10)	2778(3)	4580(2)	2085(1)	37(1)
C(11)	1793(3)	4446(2)	2078(2)	49(1)
C(12)	1268(3)	4959(3)	2320(2)	64(1)
C(13)	1732(4)	5600(3)	2580(2)	65(1)
C(14)	2717(4)	5736(2)	2608(2)	59(1)
C(15)	3237(3)	5239(2)	2355(2)	46(1)
C(20)	4094(3)	4479(2)	1381(1)	40(1)
C(21)	3714(3)	5196(2)	1185(2)	52(1)
C(22)	4162(4)	5625(3)	852(2)	66(1)
C(23)	4984(4)	5342(3)	714(2)	74(2)
C(24)	5359(4)	4630(3)	896(2)	68(1)
C(25)	4923(3)	4198(3)	1231(2)	51(1)
C(30)	4009(3)	3132(2)	3372(1)	41(1)
C(31)	4259(5)	2660(3)	3817(2)	90(2)
C(32)	3958(5)	2831(4)	4279(2)	93(2)
C(33)	3397(4)	3464(3)	4298(2)	68(1)
C(34)	3122(4)	3928(3)	3860(2)	69(1)
C(35)	3427(3)	3763(3)	3395(2)	55(1)
C(40)	5812(3)	2764(2)	3150(1)	38(1)
C(41)	6320(3)	2077(2)	3152(2)	46(1)
C(42)	7306(3)	2014(2)	3429(2)	56(1)
C(43)	7802(3)	2633(3)	706(2)	61(1)
C(44)	7303(3)	3327(3)	710(2)	66(1)
C(45)	6312(3)	3391(2)	3432(2)	55(1)
C(50)	1630(3)	926(2)	1569(1)	39(1)
C(51)	693(3)	1238(3)	1449(2)	59(1)
C(52)	−129(4)	789(3)	1473(2)	74(1)
C(53)	−3(4)	24(3)	1629(2)	65(1)
C(54)	928(4)	−281(3)	1763(2)	66(1)
C(55)	1746(3)	164(2)	1732(2)	57(1)
C(60)	3151(3)	811(2)	1036(2)	43(1)
C(61)	4133(3)	585(3)	1121(2)	62(1)
C(62)	4435(4)	95(3)	763(3)	84(2)
C(63)	3753(5)	−185(3)	326(2)	88(2)
C(64)	2783(5)	23(3)	235(2)	78(2)
C(65)	2468(4)	521(3)	587(2)	61(1)
C(70)	1819(3)	2053(3)	2890(2)	52(1)
C(71)	2147(7)	1511(4)	3265(3)	150(4)
C(72)	1622(10)	1319(4)	3641(4)	189(6)
C(73)	773(7)	1677(6)	3647(3)	143(4)
C(74)	497(6)	2242(7)	3305(4)	186(5)
C(75)	1003(5)	2433(6)	2932(3)	144(4)
C(80)	1441(3)	4102(2)	537(2)	48(1)
C(81)	2017(4)	4177(3)	167(2)	67(1)
C(82)	2074(4)	4905(4)	−70(2)	83(2)
C(83)	1589(4)	5533(3)	62(2)	83(2)
C(84)	1034(4)	5468(3)	429(2)	77(2)
C(85)	958(3)	4752(3)	666(2)	62(1)
C(90)	811(3)	2493(2)	315(2)	48(1)
C(91)	−134(4)	2226(3)	259(2)	69(1)
C(92)	−537(4)	1665(4)	−120(2)	89(2)
C(93)	3(5)	1381(3)	−449(2)	88(2)
C(94)	925(5)	1670(4)	−415(2)	105(2)
C(95)	1346(4)	2210(3)	−27(2)	81(2)
C(100)	−1070(3)	3460(3)	1633(2)	50(1)
C(101)	−1315(5)	2862(3)	1930(2)	86(2)
C(102)	−2085(6)	2968(5)	2190(3)	117(3)
C(103)	−2563(5)	3652(6)	2155(3)	114(3)
C(104)	−2325(5)	4231(5)	1864(3)	117(3)
C(105)	−1590(4)	4141(4)	1601(2)	85(2)
C(200)	3591(6)	7232(5)	4281(3)	130(3)
Cl(1)	2955(2)	6412(1)	4052(1)	134(1)
Cl(2)	3251(3)	7704(2)	4766(1)	219(2)

U_{eq} is defined as one third of the trace of the orthogonalized U_{ij} tensor.

spectively. A complete list of bond lengths and angles and tables of hydrogen atom coordinates and anisotropic thermal parameters have been deposited with the Cambridge Crystallographic Data Centre.

3. Results and discussion

3.1. Synthesis

As previously described [9], photolysis of a toluene solution of $[Fe_2(CO)_7(\mu\text{-dppm})]$ and one equivalent of $Ph_2PC{\equiv}CPh$ for 2 h afforded orange $[Fe_2(CO)_4(\mu\text{-}C{\equiv}CPh)(\mu\text{-}PPh_2)(\mu\text{-dppm})]$ **1**. If the photolysis time was extended it was noted that a small amount of a second red complex formed which proved difficult to separate from **1** by chromatography. Further, if more than one equivalent of the alkynyl phosphine was used, the yield of this second complex increased. The identity of this second product was found to be $[Fe_2(CO)_3(Ph_2PC{\equiv}CPh)(\mu\text{-}C{\equiv}CPh)(\mu\text{-}PPh_2)(\mu\text{-dppm})]$ **2**, which was also formed in ca. 70% yield upon photolysis of a toluene solution of **1** and $Ph_2PC{\equiv}CPh$ for 12 h while purging with nitrogen. While **1** and **2** were difficult to separate by chromatography, crystallisation of a mixture upon slow diffusion of methanol into a dichloromethane solution afforded large orange and red crystals of **1** and **2** respectively, which were easily separated by hand. Somewhat surprisingly, it was noted that thermolysis of a xylene solution of **2** for 2 h resulted in the clean formation of **1** in 66% yield, presumably as a result of loss of the coordinated alkynyl phosphine and carbonyl scavenging.

The triethylphosphite complex $[Fe_2(CO)_3\{P(OEt)_3\}(\mu\text{-}C{\equiv}CPh)(\mu\text{-}PPh_2)(\mu\text{-}dppm)]$ **3** was prepared in 52% yield upon thermolysis of **1** and a slight excess of the phosphite in toluene for 2 h. No evidence was seen for phosphite addition to the acetylide moiety, as previously found for hexacarbonyl $[Fe_2(CO)_6(\mu\text{-}C{\equiv}CPh)(\mu\text{-}PPh_2)]$ [11]. Likewise, thermolysis of **1** with a range of primary and secondary amines did not result in any discernable reaction, which is in marked contrast to the reactivity of the hexacarbonyl complexes [12]. This suggests that incorporation of the diphosphine renders the acetylide moiety in **1** less electrophilic, that is less susceptible to attack by nucleophiles. In support of this, and adding weight to an electronic rather than a steric effect for this marked change in reactivity, we have found that acids add readily to **1**, while even at low pH $[Fe_2(CO)_6(\mu\text{-}C{\equiv}CPh)(\mu\text{-}PPh_2)]$ does not undergo reaction with acids [13].

3.2. Characterising data

Complexes **1–3** were easily characterised on the basis of analytical and spectroscopic data. Molecular ions are seen in their positive-ion FAB mass spectra, together with peaks associated with loss of one or more carbonyl ligands. IR spectra proved diagnostic of the number of carbonyl ligands, with the highest frequency carbonyl absorptions being observed at 1991 cm^{-1} in tetracarbonyl **1**, and 1953 and 1957 cm^{-1} in tricarbonyls **2** and **3** respectively. For **2**, a weak band at 2180 cm^{-1} is assigned to the free carbon–carbon triple bond, while for both **2** and **3** four further absorptions were seen, one of which is presumably due to the metal-bound acetylide ligand. For **1** and **2**, ^1H NMR spectra yielded little information, simply consisting of complex sets of aromatic multiplets and inequivalent methylene protons. For **3**, the diastereotopic nature of the methylene protons of the phosphite was clearly evidenced by the presence of complex multiplets at δ 3.81 and 3.50 ppm, the second overlapping with one of the methylene signals of the dppm ligand.

Most informative in all cases was the ^{31}P NMR spectrum. At room temperature, the spectrum of **1** simply consists of a low-field triplet and a high-field doublet assigned to phosphido and diphosphine ligands respectively, being indicative of fast acetylide fluxionality on the NMR timescale. For both **2** and **3**, four resonances are observed at room temperature and above, indicating that acetylide fluxionality is slow. The low-field phosphido-bridge resonance appears as a doublet of doublet of doublets, couplings to the diphosphine of between 80 and 140 Hz being indicative of a *trans* arrangement of these ligands. In **2**, the alkynyl phosphine appears as a doublet (J 29.9 Hz) at 55.5 ppm, being coupled only to the phosphido-bridge, while for **3**, the phosphite is seen as a doublet of doublets (J 38.5, 16.0 Hz) at 190.4 ppm, the larger coupling being to the phosphido-bridge and the smaller to one end of the diphosphine. In the ^{13}C NMR spectrum, both **2** and **3** show three inequivalent carbonyl signals, a complex multiplet in the aromatic region and a signal at about 40 ppm assigned to the methylene carbon of dppm. For **3**, α- and β-carbons of the acetylide ligand are clearly seen at 100.39 (d, J 8.7 Hz) and 68.12 (s) ppm respectively, however, for **2** the situation is more complex. Based on a comparison of ^{13}C NMR data for the related diruthenium complex *cis*-$[Ru_2(CO)_5(Ph_2PC{\equiv}CBu^t)(\mu\text{-}C{\equiv}CBu^t)(\mu\text{-}PPh_2)]$ [14], we tentatively assign resonances at 105.3 (d, J 8.0 Hz) and 100.7 (s) to C_α and C_β of the acetylide ligand respectively, and 91.2 (d, J 30.0 Hz) and 122.4 (s) to the α- and β-carbons of the alkynyl phosphine. It is noteworthy, however, that in the related diruthenium complex coupling constants of 86.2 and 11.9 Hz were reported to C_α and C_β respectively [14].

3.3. X-ray crystal structures of $[Fe_2(CO)_4(\mu\text{-}C{\equiv}CPh)(\mu\text{-}PPh_2)(\mu\text{-}dppm)]$ 1 and $[Fe_2(CO)_3(Ph_2PC{\equiv}CPh)(\mu\text{-}C{\equiv}CPh)(\mu\text{-}PPh_2)(\mu\text{-}dppm)]$ 2

The results of single-crystal X-ray diffraction studies carried out on **1** and **2** are shown in Figs. 1 and 2 respectively, while Table 4 gives selected bond lengths and angles for both and $[Fe_2(CO)_{6-n}(PPh_3)_n(\mu\text{-}$

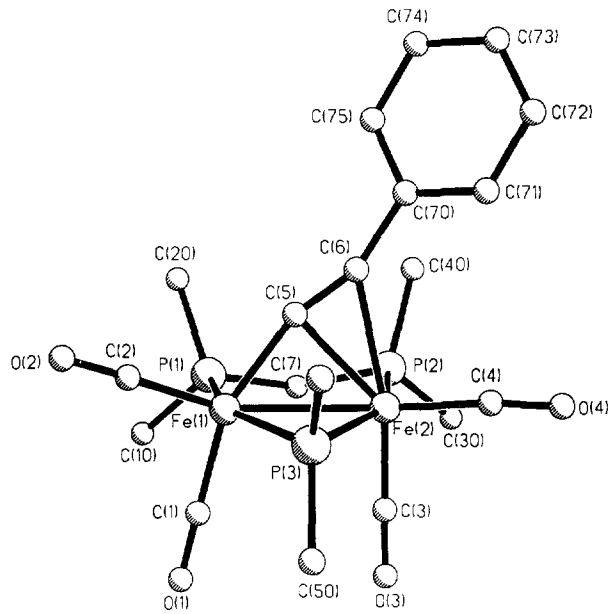

Fig. 1. Molecular structure of **1** (phenyl groups of the phosphine ligands omitted for clarity) with selected bond lengths (Å) and angles (°): Fe(1)–C(1) 1.768(4), Fe(1)–C(2) 1.760(4), Fe(2)–C(3) 1.740(4), Fe(2)–C(4) 1.766(4); Fe(1)–C(5)–Fe(2) 80.58(13), Fe(1)–C(5)–C(6) 160.8(3), C(5)–C(6)–C(70) 158.8(4), C(1)–Fe(1)–Fe(2) 104.64(12), C(2)–Fe(1)–Fe(2) 150.24(12), C(3)–Fe(2)–Fe(1) 90.77(12), C(4)–Fe(2)–Fe(1) 157.66(12).

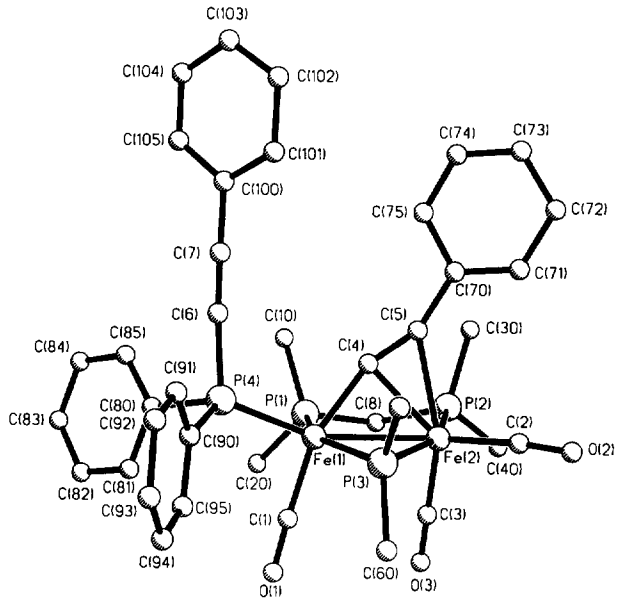

Fig. 2. Molecular structure of **2** (phenyl groups of the phosphine ligands omitted for clarity) with selected bond lengths (Å) and angles (°): Fe(1)–P(4) 2.196(1), Fe(1)–C(1) 1.764(4), Fe(2)–C(2) 1.765(4), Fe(2)–C(3) 1.740(4); Fe(1)–C(4)–Fe(2) 80.56(13), Fe(1)–C(4)–C(5) 159.5(3), C(4)–C(5)–C(70) 156.2(4), C(1)–Fe(1)–Fe(2) 107.49(12), C(2)–Fe(2)–Fe(1) 152.38(12), C(3)–Fe(2)–Fe(1) 84.45(12).

$C{\equiv}CPh)(\mu\text{-}PPh_2)]$ (n = 0 [6], 1[7]). Within the series, the iron–iron bond length at approximately 2.59 Å is essentially invariant for **1**, **2** and the hexacarbonyl, while in contrast that of 2.648(1) Å in the pentacarbonyl complex is elongated somewhat. In the latter, the monodentate phosphine lies approximately *cis* to the metal–metal bond and *trans* to the phosphido-bridge, a position occupied by the diphosphine in **1** and **2**. Inclusion of dppm, however, does not alter the central core geometry of the molecule, as is also highlighted by the very small differences in the angle at the phosphido-bridge upon its inclusion. Further, since **2** contains a phosphine approximately *trans* to the metal–metal vector [P(4)–Fe(1)–Fe(2) 151.03(4)°] and thus expected to display a strong σ-inductive effect, this suggests that the steric and electronic requirements of the diphosphine override the σ-inductive effect of the monodentate phosphine. In all four structures the phenyl acetylide ligand bridges the diiron vector being σ-bound to one metal centre and π-bound to the second, and the carbon–carbon bond of approximately 1.23 Å and does not vary significantly, while the unbound carbon–carbon triple bond of the alkynyl phosphine in **2** at 1.206(5) Å is slightly shorter as expected.

Table 4
Selected crystallographic data for diiron acetylide complexes

	1	2	$(CO)_6$	$(CO)_5$
Fe(1)–Fe(2)	2.5882(9)	2.5958(10)	2.597(2)	2.648(1)
Fe(1)–P(1)	2.215(1)	2.244(1)	—	2.274(1)
Fe(2)–P(2)	2.243(1)	2.235(1)	—	—
Fe(1)–P(3)	2.034(1)	2.231(1)	2.213(2)	2.212(1)
Fe(2)–P(3)	2.058(1)	2.218(3)	2.224(2)	2.233(1)
Fe(1)–C_α	1.884(4)	1.881(3)	1.891(6)	1.890(4)
Fe(2)–C_α	2.109(3)	2.124(3)	2.125(9)	2.116(4)
Fe(2)–C_β	2.304(4)	2.290(4)	2.304(7)	2.284(5)
C_α–C_β	1.229(4)	1.242(5)	1.232(10)	1.225(6)
Fe(1)–P(3)–Fe(2)	71.88(4)	71.38(3)	71.64(7)	73.1(0)
ΔC_α	0.225	0.243	0.234	0.226

$(CO)_6 = [Fe_2(CO)_6(\mu\text{-}C{\equiv}CPh)(\mu\text{-}PPh_2)]$.
$(CO)_5 = [Fe_2(CO)_5(PPh_3)(\mu\text{-}C{\equiv}CPh)(\mu\text{-}PPh_2)]$.

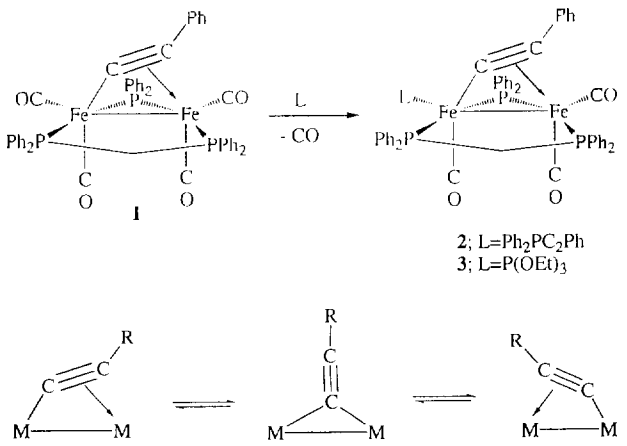

Scheme 1. σ – π Acetylide fluxionality.

As shown in Scheme 1, acetylide fluxionality is proposed to occur via a linear transition state (or intermediate) in which the α-carbon is bound symmetrically to both metal centres, while the β-carbon is released from both (Scheme 1). Based on these criteria we might anticipate that (with all other things being equal) the more symmetrical the binding of C_α in the ground state and the longer the iron–C_β bond, the lower the free energy of activation for the fluxional process. A comparison of ΔC_α values for the four complexes reveals that they differ by a maximum of only 0.018 Å, while Fe–C_β distances vary by 0.020 Å, the longest at 2.304 Å being found for both **1** and $[Fe_2(CO)_6(\mu\text{-}C{\equiv}CPh)(\mu\text{-}PPh_2)]$. Further, since the ΔC_α value at 0.225 Å in **1** varies only slightly from that of the hexacarbonyl (0.234 Å) it is difficult to equate these small ground state effects with the moderate decrease in $\Delta G^{\#}$ of about 1 Kcal mol^{-1} upon coordination of dppm. This suggests, then, that other effects are responsible for this difference, the most likely being the stabilisation of the developing positive charge at the α-carbon of the acetylide by the electron-releasing diphosphine. Based on the last premise, acetylide fluxionality in **2** might be anticipated to have a low free energy of activation. Clearly, however, as inspection of Fig. 3 reveals, the alkynyl phosphine sterically blocks the fluxional process. It is of interest to note that acetylide fluxionality does still occur in $[Fe_2(CO)_5(PPh_3)(\mu\text{-}C{\equiv}CPh)(\mu\text{-}$

PPh_2)] [4], but here it must be associated with a trigonal rotation (twist) of the $Fe(CO)_2(PPh_3)$ unit, thus easing the steric demands of the phosphine ligand. Clearly in **2**, the presence of the diphosphine prevents such a trigonal rotation and thus acetylide mobility is curtailed. It is noteworthy, however, that based on the discussion above, an isomer of **2** in which P(4) and C(1) are interchanged might be expected to display high mobility of the acetylide ligand. To date, however, we have not been able to prepare this.

4. Conclusions

This work has shown that simple phosphine and phosphite derivatives of $[Fe_2(CO)_4(\mu\text{-}C{\equiv}CPh)(\mu\text{-}PPh_2)(\mu\text{-dppm})]$ **1** can be prepared in which the $\sigma-\pi$ acetylide fluxionality, so facile in **1**, is frozen out. An examination of the solid state structures of four diiron phenyl acetylide complexes does not reveal any substantial change in the nature of the acetylide binding upon successive carbonyl substitutions. This suggests that other factors, namely the electronic stabilisation of the transition state by better donor ligands and adverse steric interactions, can lead to a decrease or increase respectively in the free energy of activation for the fluxional process.

Acknowledgements

We would like to thank EPSRC for a studentship to S.P.R. and Dr. S. Doherty for kindly providing a sample of $Ph_2PC{\equiv}CPh$.

References

[1] R. Nast, *Coord. Chem. Rev., 47* (1982) 89; A.J. Carty, *Pure Appl. Chem., 54* (1982) 113; P.R. Raithby and M.J. Rosales, *Adv. Inorg. Radiochem., 29* (1986) 169.
[2] A.A. Cherkas, *Ph.D. Thesis*, University of Waterloo, 1989; K. Lee, W.T. Pennington, A.W. Cordes and T.L. Brown, *J. Am. Chem. Soc., 107* (1985) 631; R.J. Mercer, M. Green and A.G. Orpen, *J. Chem. Soc., Chem. Commun.*, (1986) 567; R.W.M. Ten Hoedt, G. Van Koten and J.G. Noltes, *J. Organomet. Chem., 133* (1977) 173; R.W.N. Hoedt, J.G. Noltes, G. Van Koten and A.L. Spek, *J. Chem. Soc., Dalton Trans.*, (1978) 1800.
[3] A.A. Cherkas, L.H. Randall, S.A. MacLaughlin, G.N. Mott, N.J. Taylor and A.J. Carty, *Organometallics, 7* (1988) 964.
[4] L.H. Randall, *Ph.D. Thesis*, University of Waterloo, 1991.
[5] G. Hogarth, M.H. Lavender and K. Shukri, *J. Organomet. Chem., 527* (1997) 247.
[6] H.A. Patel, R.G. Fischer, A.J. Carty, D.V. Naik and G.J. Palenik, *J. Organomet. Chem., 60* (1973) C19.
[7] W.F. Smith, J. Yule, N.J. Taylor, H.N. Paik and A.J. Carty, *Inorg. Chem., 16* (1977) 1593.
[8] A.J. Carty, N.K. Hota, T.W. Ng, H.A. Patel and T.J. Conner, *Can. J. Chem.*, (1971) 2706.
[9] A.A. Cherkas, S. Doherty, M. Cleroux, G. Hogarth, L.H. Randall, S.M. Breckenridge, N.J. Taylor and A.J. Carty, *Organometallics, 11* (1992) 1701.
[10] G.M. Sheldrick, SHELXTL-93, *Program package for structure solution and refinement*, Siemens Analytical Instruments Inc., Madison, WI, 1993.
[11] Y.S. Wong, H.N. Paik, P.C. Chieh and A.J. Carty, *J. Chem. Soc., Chem. Commun.*, (1975) 309.
[12] A.A. Cherkas, G.N. Mott, R. Granby, S.A. MacLaughlin, J.E. Yule, N.J. Taylor and A.J. Carty, *Organometallics, 7* (1988) 1115; A.A. Cherkas, L.H. Randall, N.J. Taylor, G.N. Mott, J.E. Yule, J.L. Guinamant and A.J. Carty, *Organometallics, 9* (1990) 1677; A.J. Carty and G.N. Mott, *Inorg. Chem., 22* (1983) 2726.
[13] G. Hogarth, unpublished results.
[14] A.J. Carty, A.A. Cherkas and L.H. Randall, *Polyhedron, 7* (1988) 1045.